Energy Proceedings
Vol 36, 2023
ISSN 2004-2965

Identification and localization of Photovoltaic Defect from UAV Thermal Infrared Data Based on Photogrammetry and Deep Learning

Bo Wang[1*], Mengmeng Wang[1*], Xiaodan Shi[2], Qi Chen[1], Jian Yang[1], Zhengjia Zhang[1]

1 School of Geography and Information Engineering, China University of Geosciences (Wuhan), Wuhan 430074, China;

2 Center for Spatial Information Science, the University of Tokyo, Japan;
*Corresponding Author: wangbobby1026@cug.edu.cn (B.W.); wangmm@cug.edu.cn (M.W.)

ABSTRACT

This study presents an efficient framework for locating and classifying faulty Photovoltaic (PV) panels from Unmanned Aerial Vehicle (UAV) thermal infrared images. First, aerial triangulation based on photogrammetry is used to obtain thermal infrared images of PV panels with coordinate information, then, individual PV panels are segmented based on High-Resolution Network (HRNetV2-W32), finally, the panels are fed into residual net (ResNet-50) to classify the fault types. Results showed that the panel segmentation accuracy reaches 98.54%, the classification accuracy reaches 88.74%, and the coordinate error is better than 0.033m.

Keywords: Photovoltaic, Deep Learning, Semantic Segmentation, Defect Classification, Thermal Infrared

NONMENCLATURE

Abbreviations	
PV	Photovoltaic
UAV	Unmanned Aerial Vehicle
HRNet	High-Resolution Network
TIRDOM	Thermal Infrared Digital Orthophoto Map
CNN	Convolutional Neural Networks
Symbols	
m	Meter
s	Second

1. INTRODUCTION

In recent years, the photovoltaic power generation has grown exponentially, and the global photovoltaic panel construction and power generation are showing a blowout trend[1]. Designed life of photovoltaic power plants is 25-30 years, during which time defects will inevitably occur. The defects may reduce power generation, shorten battery life, and cause panel burnout in severe cases. Therefore, timely detection of photovoltaic panel defects can promote the safe and efficient operation of photovoltaic power plants[2].

There are two types of fault detection for solar panels: detection based on electrical signals (current and voltage) and detection based on images (vision)[3, 4]. Thermal infrared images with a resolution of up to 0.02 m have proven to be sufficient for detecting defect types in practical applications, and thermal infrared photos with a resolution of 0.02 m are more efficient at the photographic stage than millimeter-scale RGB images. With the development of deep learning technology, more and more research utilized deep learning algorithms to panel segmentation and photovoltaic fault identification from thermal infrared images, including VGG-16, Mask R-CNN, etc[5, 6]. They have been effective at categorizing specific photos or using masks to detect problematic cells on photographs, but they have been unsuccessful in segmenting into different kinds of defects and have only segmented overheated panels. In addition, it is also important to locate defective panels in practical applications. A study has used the Structure from Motion - MultiView Stereo (SfM-MVS) to acquire electric field orthophotos, segment PV panels based on geometric features, and use convolutional neural networks to detect and classify panel faults[7]. However, the detected types do not clearly reflect the true electrical fault characteristics or indicate the cause of the fault.

In this study, the thermal infrared camera mounted on a UAV with Real-time kinematic (RTK) and inertial motion unit (IMU) was used to take images of PV plants.

This is a paper for the 9th Applied Energy Symposium: Low Carbon Cities and Urban Energy Systems (CUE2023), Sep. 2-7, 2023, Matsue & Tokyo, Japan.

The aerial triangulation was employed to generate thermal infrared Digital Orthophoto Map (TIRDOM), and then HRNetV2-W32 and ResNet-50 deep learning models were used to segment individual PV panel images and classify panel fault types, respectively, to obtain panel information with high-precision coordinates and faulty types. Six power stations in Guangzhou were used to assess the performance of the proposed method.

2. DATASET ACQUISITION AND METHODS

The technical route of this paper is shown in Fig.1: first, the data acquisition and pre-processing stage, using the thermal infrared camera on the UAV to capture the photos of the PV plant, based on the photogrammetry algorithm to process the photos to generate the TIRDOM of the PV plant; secondly, the PV panel segmentation stage, using the semantic segmentation algorithm to segment the TIRDOM into a binarized mask of the PV panel and the background, using the mask to crop the PV panels on the TIRDOM into separate panel images; finally, using the classification model to classify the defects of the PV panels.

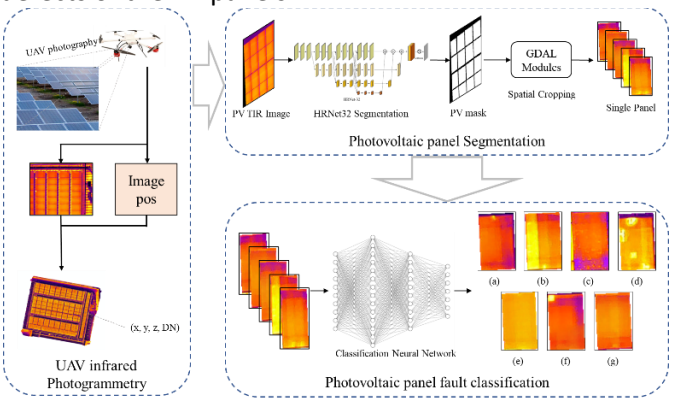

Fig.1 Photovoltaic panel defect location and classification framework technical route

2.1 Data acquisition and orthophoto production

The data acquisition mission was performed on clear and cloudless days, with vertical panel shots that would allow the thermal infrared sensor to pick up the maximum amount of radiation from the PV panels; the heading and lateral overlap were set to 80% and 75%, respectively. The camera used was a DJI Zenmuse H20T equipped with an RGB with a laser ranging module and a thermal infrared camera (TIR), with the specific parameters of the thermal infrared sensor shown in Table 1. The camera-equipped UAV is a DJI MATRICE 300 RTK, which provides highly accurate POS information. A total of 189,632 images were taken from the six power stations in Guangzhou, Guangdong Province, China (Lon: 112°57' - 114°3', Lat: 22°26' - 32°56') with a combined capacity of 700 MW.

Table.1 H20T thermal infrared sensor parameters

Thermal infrared sensor types	Uncooled Vanadium Oxide (VOx) Microbolometer
DFOV	40.6°
Focal length	13.5 mm
Temperature measurement range	-40℃ to 150℃ (high gain mode) -40℃ to 550℃ (low gain mode)
Sensitivity (NETD)	≤50 mK @ f/1.0
Photo resolution	640×512

To obtain the coordinate information of the photovoltaic panel, we use PhotoScan to read the photo information, add the ground control point correction model after aerial triangulation, and finally generate a high-precision thermal infrared orthophoto.

2.2 Photovoltaic fault detection algorithm

In order to locate the position of the photovoltaic panel and classify the types of defects and faults more easily, it is necessary to segment the PV panels from the middle image using semantic segmentation networks. Most semantic segmentation networks use convolutional neural networks (CNN) to extract image features in the encoder stage and transposed convolution to restore the images to their original resolution in the decoder stage, such as U-Net, DeconvNet, etc[8, 9]. This will lose some information from the original high-resolution image, which will reduce the accuracy of segmentation. This study employed the HRNetV2-W32 network as the segmentation network to maintain the high-resolution image's original information and enhance segmentation pixel accuracy[10]. By connecting image features from different resolutions in parallel to create interaction between image features from different resolutions, HRNet maintains the features from high-resolution images. First, feature vectors from images with four different resolutions are extracted using convolutional layers of different resolutions; then, these feature vectors are unified to the maximum resolution by 1×1 convolutional layers and summed; finally, a softmax linear classifier is used to predict the segmentation map.

The training set contains 18,000 PV panels, of which 10,000 panels were taken from the power plant with the highest spatial resolution (0.018 m) and the remaining 8,000 panels were randomly selected from the other five power plants. Dice loss was chosen as the loss function of the optimizer, which is a function that measures the similarity of two samples and takes values in the range of 0-1, with the formula：

$$s = \frac{2|X \cap Y|}{|X| + |Y|} \quad (1)$$

where, $|X \cap Y|$ represents the intersection of X and Y, $|X|$ and $|Y|$ represent the number of elements of X and Y.

Different defect types can provide suggestions for post-maintenance of Photovoltaic power plants, and the classification of PV panel defects based on thermal infrared images is essential. In this section, ResNet-50 was chosen as the classification network model because it has high accuracy performance on the ImageNet dataset by rewriting its fully connected layer to output a 1×7 vector output[11].

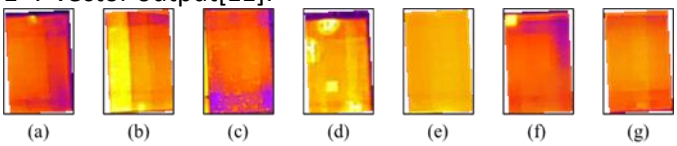

Fig.2 Panel type, (a) Bypass diode operation, (b) Group string open circuit, (c) Clutter covering, (d) Panel breakage, (e) Dusty, (f) General hot spot, (g) Normal Panel

Production of classification data sets: after segmentation, the resolution of most panels did not exceed 70 pixels, and the image size of photovoltaic panels was resampled to 64×64 pixels for the convenience of network training. The fault type is shown in Fig.2. The test set randomly selected 10% of images from each type of dataset for accuracy validation, and the remaining 90% of samples were randomly selected by the algorithm in each epoch, with a ratio of 8:2 between the training and validation sets. In network training, random flips and rotations were used for image enhancement, an Adam optimizer was selected to update the network weights, and a cross-entropy loss function was used as a loss to evaluate the classification accuracy of the model. In the multi-classification method, the cross-entropy loss function is:

$$L = -\frac{1}{N}\sum_{i}\sum_{c=1}^{M} y_{ic}\log(p_{ic}) \tag{2}$$

where, M denotes the number of categories; y_ic is the sign function, which is 1 when the true category of sample i is equal to c and 0 otherwise; p_ic is the probability that sample i belongs to category c.

The segmentation result accuracy verification selected the intersection of union (IoU), precision, recall, and f1 score to measure, and the calculation method is as follows:

$$IoU = \frac{TP}{TP + FN + FP} \tag{3}$$

$$Precision = \frac{TP}{TP + FP} \tag{4}$$

$$Recall = \frac{TP}{TP + FN} \tag{5}$$

$$F1\ Score = \frac{2 \times precision \times recall}{precision + recall} \tag{6}$$

where, TP (True Positive) is the image element that is predicted correctly, FP (False Positive) is the image element that divides the background into PV panels, and FN (False Negative) is the image element that divides the PV panels into the background.

Classification accuracy was evaluated using overall accuracy (OA) and Kappa coefficient, calculated as:

$$OA = \frac{1}{N}\sum_{i=1}^{r} x_{ii} \tag{7}$$

$$Kappa = \frac{N\sum_{i=1}^{r} x_{ii} - \sum_{i=1}^{r}(x_{i+} \times x_{+i})}{N^2 - \sum_{i=1}^{r}(x_{i+} \times x_{+i})} \tag{8}$$

where, N is the total number of samples, x_{ii} is the number of samples labeled as class i that were assigned to class i, x_{i+} is the number of samples labeled as class i, and x_{+i} is the number of samples assigned to class i.

3. RESULTS

In the positioning accuracy verification, the Baiyun Electric Equipment Co. (RGB DOM spatial resolution 0.007m, TIRDOM spatial resolution 0.018m) was selected as the verification area, and the visible DOM (horizontal positioning accuracy better than 0.03m) was generated after aerial triangulation of the visible image corrected by ground control points as a reference to verify the positioning error of thermal infrared DOM on the PV panel. We evenly selected 9 points on the DOM of the whole power plant as validation points. It is verified that the maximum error of horizontal positioning in the PV panel positioning stage is 0.257m for x and 0.123m for y, which means the positioning error is less than 0.33m.

In the panel segmentation, the test set was selected from two different aerial height photovoltaic panels, as Fig.3 illustrated, where (1) (2) are photovoltaic panel images with spatial resolution of 0.018m, 0.024m, (a) (b) (c) are TIRDOM, binarized mask images after semantic segmentation, and overlapping images with the TIRDOM after vectorization of the mask image. According to Table.2, the precision of image segmentation with spatial resolution of 0.018m is 98.54%, and IoU is 95.73%. The precision of image segmentation with spatial resolution of 0.024m is 93.60%, and IoU is 92.61%.

The classification results are shown in Table.3. It can be seen that using ResNet-50 to classify photovoltaic defects, the OA is 88.74% and the Kappa accuracy is 0.86. Among them, group string open circuit, panel breakage, dust, and normal panel accuracy are reached 100%, the accuracy of bypass diode operation is 83.33%, the

accuracy of clutter covering is 36.84%, and the accuracy of general hot spot is 91.1%. Some of the highlights that were either too large or too little were classified as general hot spots or noise of typical panels, which lead to poor clutter coverage accuracy.

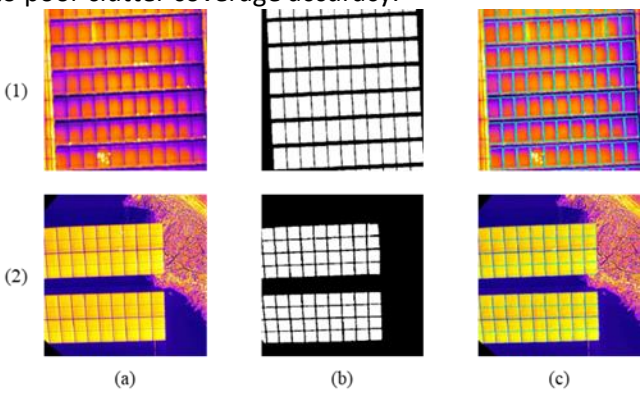

Fig.3 Test set split results

Tabel.2 Panel segmentation accuracy

	Spatial resolution	IoU	Precision	Recall	F1 Score
Test	0.018m	95.73%	98.54%	97.10%	97.81%
Test	0.024m	92.61%	93.60%	98.87%	96.16%

Tabel.3 Panel segmentation accuracy

Model	Parameters	Training time	OA	Kappa
ResNet-50	25.7M	1104.53s	88.74%	0.86

4. CONCLUSIONS

The method proposed in this paper can accurately locate the defects of PV panels and classify the defect types, providing reference on defective panels for PV power plants to facilitate their operation and maintenance. After segmentation, the center of the panel is used as the localization point, and the localization error is less than 0.33m with a spatial resolution of 0.018m and no ground control points, which can ensure that the localization point of defective panels is within the panel relative to PV panels with length and width larger than 1m; the f1-score of panel segmentation surpassed 95%, illustrating the model could accurately segment most of the PV panels. The accuracy of ResNet-50 in the defect classification stage is 88.74%.

REFERENCE

[1] Alwar S, Samithas D, Boominathan MS, Balachandran PK, Mihet-Popa L. Performance Analysis of Thermal Image Processing-Based Photovoltaic Fault Detection and PV Array Reconfiguration-A Detailed Experimentation. Energies. 2022;15.

[2] Hernandez-Callejo L, Gallardo-Saavedra S, Alonso-Gomez V. A review of photovoltaic systems: Design, operation and maintenance. Solar Energy. 2019; 188: 426-40.

[3] Triki-Lahiani A, Bennani-Ben Abdelghani A, Slama-Belkhodja I. Fault detection and monitoring systems for photovoltaic installations: A review. Renewable & Sustainable Energy Reviews. 2018;82:2680-92.

[4] Meng ZY, Xu SZ, Wang LC, Gong YK, Zhang XD, Zhao Y. Defect object detection algorithm for electroluminescence image defects of photovoltaic modules based on deep learning. Energy Science & Engineering. 2022;10:800-13.

[5] Pierdicca R, Malinverni ES, Piccinini F, Paolanti M, Felicetti A, Zingaretti P. DEEP CONVOLUTIONAL NEURAL NETWORK FOR AUTOMATIC DETECTION OF DAMAGED PHOTOVOLTAIC CELLS. Int Arch Photogramm Remote Sens Spatial Inf Sci. 2018;XLII-2:893-900.

[6] Pierdicca R, Paolanti M, Felicetti A, Piccinini F, Zingaretti P. Automatic Faults Detection of Photovoltaic Farms: solAIr, a Deep Learning-Based System for Thermal Images. Energies. 2020;13.

[7] Zefri Y, Sebari I, Hajji H, Aniba G. Developing a deep learning-based layer-3 solution for thermal infrared large-scale photovoltaic module inspection from orthorectified big UAV imagery data. International Journal of Applied Earth Observation and Geoinformation. 2022;106.

[8] Ronneberger O, Fischer P, Brox T. U-Net: Convolutional Networks for Biomedical Image Segmentation. Medical Image Computing and Computer-Assisted Intervention – MICCAI 20152015. p. 234-41.

[9] Noh H, Hong S, Han B, Ieee. Learning Deconvolution Network for Semantic Segmentation. IEEE International Conference on Computer Vision. Santiago, CHILE2015. p. 1520-8.

[10] Wang JD, Sun K, Cheng TH, Jiang BR, Deng CR, Zhao Y, et al. Deep High-Resolution Representation Learning for Visual Recognition. Ieee Transactions on Pattern Analysis and Machine Intelligence. 2021;43:3349-64.

[11] He K, Zhang X, Ren S, Sun J. Deep residual learning for image recognition. Proceedings of the IEEE conference on computer vision and pattern recognition2016. p. 770-8.